Supramolecular Assemblies of a New Series of Gemini-Type Schiff Base Amphiphiles at the Air/Water Interface: In Situ Coordination, Interfacial Nanoarchitectures, and Spacer Effect

ARTICLE *in* LANGMUIR · JUNE 2006

Impact Factor: 4.46 · DOI: 10.1021/la060343w · Source: PubMed

2 AUTHORS:

Tifeng Jiao
Yan Shan University
106 PUBLICATIONS **530** CITATIONS
SEE PROFILE

Minghua Liu
Chinese Academy of Sciences
246 PUBLICATIONS **5,195** CITATIONS
SEE PROFILE

Supramolecular Assemblies of a New Series of Gemini-Type Schiff Base Amphiphiles at the Air/Water Interface: In Situ Coordination, Interfacial Nanoarchitectures, and Spacer Effect

Tifeng Jiao and Minghua Liu*

Beijing National Laboratory for Molecular Sciences (BNLMS), CAS Key Laboratory of Colloid and Interface Science, Institute of Chemistry, The Chinese Academy of Sciences, Beijing 100080, PR China

Received February 4, 2006. In Final Form: March 13, 2006

Great interest has been devoted to the gemini amphiphiles because of their unique properties. In this article, we report some interesting properties of the interfacial films formed by a series of newly designed gemini amphiphiles containing the Schiff base moiety. This novel series of gemini amphiphiles with their Schiff base headgroups linked by a hydrophobic alkyl spacer (BisSBC18C*n*, $n = 2$, 4, 6, 8, 10) could be spread to form stable monolayers and coordinated with $Cu(Ac)_2$ in situ in the monolayer. The alkyl spacer in the amphiphiles has a great effect on the regulation of the properties of the Langmuir monolayers. A maximum limiting molecular area was observed for the monolayers of the gemini amphiphile with the spacer length of hexa- or octamethylene groups. Both the monolayers on water and on the aqueous $Cu(Ac)_2$ subphase were transferred onto solid substrates, and different morphologies were observed for films with different spacers. Nanonail and tapelike morphologies were observed for amphiphile films with shorter spacers ($n = 2$ and 4) on the water surface. Wormlike morphologies were observed for gemini films with longer spacers of C_8 and C_{10} when coordinated with $Cu(Ac)_2$. An interdigitated layer structure was supposed to form in the multilayer films transferred from water or the aqueous $Cu(Ac)_2$ subphase.

Introduction

Supramolecular architectures formed in organized systems such as monolayers,[1] Langmuir−Blodgett (LB) films,[2,3] self-assembled monolayers (SAMs),[4−6] and other systems such as vesicles and micelles[7−11] have attracted much interest. In particular, with recent advancements in nanoscience and nanotechnology, these bottom-up methods for the fabrication of nanostructures have showed some new prospects. The Langmuir−Blodgett technique is one of the sophisticated bottom-up fabrication methods for obtaining organized molecular films and is usually used in two aspects in constructing nanostructured materials. On one hand, the LB method has been used to fabricate uniform ultrathin films, which have been the central topic in the field of LB film research.[1−3] On the other hand, the formation of interfacial patterns and the construction of various nanostructures by the LB technique have also attracted great interest in recent years.[12−17] In any aspect, the selection of appropriate amphiphiles to fabricate organized molecular films is very important. So far, typical amphiphiles in which one headgroup and one or two hydrophobic chains are simultaneously contained play an important role in forming these organized architectures, and a larger amount of research on LB films has been carried out with this kind of amphiphile. Recently, two kinds of novel amphiphiles, bolaamphiphiles[18] and gemini-type amphiphiles,[19] have attracted much attention because of their unique properties not only in solution systems but also at interfaces. In this article, we report some interesting aspects of newly designed gemini-type amphiphiles. Gemini amphiphiles describe a family of amphiphiles that consist of two hydrophilic headgroups and two aliphatic chains linked by a rigid or flexible spacer unit.[20,21] Gemini amphiphiles usually have excellent foaming and wetting properties and lower critical micelle concentrations (cmc's) than the corresponding "simple" surfactants. In addition, gemini amphiphiles offer superior applications in gene transfection,[22,23]

* To whom correspondence should be addressed. E-mail: liumh@iccas.ac.cn. Tel: +86-10-82612655. Fax: +86-10-62569564.

(1) Gaines, G. L., Jr. *Insoluble Monolayers at Liquid−Gas Interfaces*; Interscience: New York, 1966.
(2) Roberts, G. G. *Langmuir−Blodgett Films*; Plenum Press: New York, 1990.
(3) Ulman, A. *An Introduction to Ultrathin Organic Films: From Langmuir−Blodgett to Self-Assembly*; Academic Press: Boston, 1991.
(4) Nuzzo, R. G.; Allara, D. L. *J. Am. Chem. Soc.* **1983**, *105*, 4481−4483.
(5) Sagiv, J. *J. Am. Chem. Soc.* **1980**, *102*, 92−98.
(6) Laibinis, P. E.; Nuzzo, R. G.; Whitesides, G. M. *J. Phys. Chem.* **1992**, *96*, 5097.
(7) Borsali, R.; Minatti, E.; Putaux, J.-L.; Schappacher, M.; Deffieux, A.; Viville, P.; Lazzaroni, R.; Narayanan, T. *Langmuir* **2003**, *19*, 6−9.
(8) Bu, W.; Li, H.; Sun, H.; Yin, S.; Wu, L. *J. Am. Chem. Soc.* **2005**, *127*, 8016−8017.
(9) Zhu, J.; Yu, H.; Jiang, W. *Macromolecules* **2005**, *38*, 7492−7501.
(10) Battaglia, G.; Ryan, A. J. *J. Am. Chem. Soc.* **2005**, *127*, 8757−8764.
(11) Benkoski, J. J.; Jesorka, A.; Kasemo, B.; Hook, F. *Macromolecules* **2005**, *38*, 3852−3860.
(12) (a) Gleiche, M.; Chi, L. F.; Fuchs, H. *Nature* **2000**, *403*, 173−175. (b) Lu, N.; Chen, X.; Molenda, D.; Naber, A.; Fuchs, H.; Talapin, D. V.; Weller, H.; Muller, J.; Lupton, J. M.; Feldmann, J.; Rogach, A.; Chi, L. *Nano Lett.* **2004**, *4*, 885−888. (c) Lu, N.; Gleiche, M.; Zheng, J.; Lenhert, S.; Chi, L.; Fuchs, H. *Adv. Mater.* **2002**, *14*, 1812−1815.
(13) (a) Lenhert, S.; Zhang, L.; Mueller, J.; Wiesmann, H. P.; Erker, G.; Fuchs, H.; Chi, L. *Adv. Mater.* **2004**, *16*, 619−623. (b) Lenhert, S.; Meier, M.-B.; Meyer, U.; Chi, L.; Wiesmann, H. P. *Biomaterials* **2005**, *26*, 563−570.
(14) (a) Gleiche, M.; Chi, L.; Gedig, E.; Fuchs, H. *ChemPhysChem.* **2001**, *3*, 187−191. (b) Zhang, M.; Lenhert, S.; Wang, M.; Chi, L.; Lu, N.; Fuchs, H.; Ming, N. *Adv. Mater.* **2004**, *16*, 409−413.
(15) (a) Pignataro, D.; Sardone, L.; Marletta, G. *Mater. Sci. Eng., C* **2002**, *22*, 177−181. (b) Pignataro, D.; Sardone, L.; Marletta, G. *Langmuir* **2003**, *19*, 5912−5917.
(16) (a) Moraille, P.; Badia, A. *Langmuir* **2002**, *18*, 4414−4419. (b) Moraille, P.; Badia, A. *Angew. Chem., Int. Ed.* **2002**, *41*, 4303−4306. (c) Moraille, P.; Badia, A. *Langmuir* **2003**, *19*, 8041−8049.
(17) Chen, P.; Gao, P.; Zhan, C.; Liu, M. *ChemPhysChem* **2005**, *6*, 1108−1113.
(18) Fuhrhop J. H.; Wang, T. *Chem. Rev.* **2004**, *104*, 2901−2938 and references therein.
(19) (a) Menger, F. M.; Littau, C. A. *J. Am. Chem. Soc.* **1991**, *113*, 1451−1452. (b) Menger, F. M.; Littau, C. A. *J. Am. Chem. Soc.* **1993**, *115*, 10083−10090. (c) Menger, F. M.; Keiper J. S. *Angew. Chem., Int. Ed.* **2000**, *39*, 1906−1920.
(20) Rosen, M. J. *Chem. Technol.* **1993**, *23*, 30.
(21) (a) Zana, R.; Benrraou, M.; Rueff, R. *Langmuir* **1991**, *7*, 1072−1075. (b) Zana, R.; Talmon, Y. *Nature* **1993**, *362*, 228. (c) Karaborni, S.; Esselink, K.; Hilbers, P. A. J.; Smit, B.; Karthaüser, J.; Van Os, N. M.; Zana, R. *Science* **1994**, *266*, 254.
(22) Jennings, K. H.; Marshall, I. C. B.; Wilkinson, M. J.; Kremer, A.; Kirby, A. J.; Camilleri, P. *Langmuir* **2002**, *18*, 2426−2429.

10.1021/la060343w CCC: $33.50
Published on Web 04/19/2006

vesicle-to-micelle transition,[24] gelators,[25,26] and templates for the preparation of nanomaterials.[27] Furthermore, they have a series of parameters such as the length of hydrophobic chains, the size of hydrophilic headgroups, the type of counterions, and the flexibility and polarity of the spacer that can induce a richer diversity of aggregate morphologies.[22−27] As a result, the special molecular geometries of gemini amphiphiles could lead to interesting aggregate structures both in solution and at the air/water interface. However, compared with the extensive investigations in solution systems, there are a fewer reports on the interfacial assemblies of gemini amphiphiles.[28−35] Different from conventional amphiphiles, the spacer in gemini amphiphiles is expected to have a great influence on the interfacial properties and the wealth of morphologies in organized films.[36−43] Previously, our group has investigated the interactions between gemini amphiphiles and DNA and observed interesting properties and surface morphologies of gemini/DNA complex films.[44] In addition, we have also designed a series of imidazole-based gemini amphiphiles and investigated their interfacial properties as well as the regulation of surface properties of the complex films of gemini/dye and gemini/polyoxometalate (POM) hybrid films.[45] In this research, we mainly designed gemini amphiphiles with positive charges and focused on the interaction between gemini amphiphiles and the species dissolved in the subphase through interfacial electrostatic interactions. In this article, we extended our work to the interfacial coordination system. We designed a series of gemini amphiphiles bearing Schiff base headgroups and investigated their coordination with metal ions in the subphase. It is well known that Schiff base derivatives are one of the important classes of organic compounds that have wide applications in biological systems and can serve as functional materials.[46] Various properties of Schiff bases, such as photochromism,[47] acidichromism,[48] coordination with metal ions,[49] and molecular recognition,[50] have been reported. Here, we designed a series of gemini amphiphiles in order to elucidate the interfacial properties of Schiff bases when they were linked by a hydrophobic spacer. We have found that the spacer of gemini amphiphiles indeed plays an important role in regulating the supramolecular assembly and coordination of the Schiff base headgroup with metal ions, resulting in great changes both in the spectra and interfacial morphologies. The interfacial behaviors and spacer effect of the organized molecular films were investigated through a series of characterization methods such as surface pressure−area isotherms, UV−vis and FTIR spectra, and atomic force microscopy (AFM) measurement.

Scheme 1. Synthetic Route and Corresponding Molecular Structures of Gemini BisSBC18C*n* Amphiphiles[a]

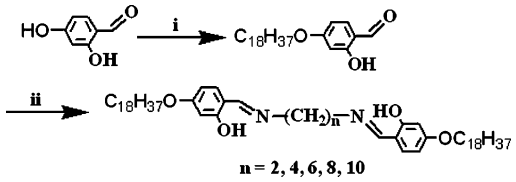

[a] (i) Potassium hydroxide, anhydrous ethanol, 1-bromooctadecane, reflux. (ii) 1,*n*-Diamine, anhydrous ethanol, reflux.

Experimental Section

Materials. 1-Bromooctadecane, 2,4-dihydroxybenzaldehyde, and diamines with various spacer lengths were obtained commercially from Aldrich, TCI, and Acros Chemicals and used as received. The solvents were obtained from Beijing Chemicals and were distilled before use. Deionized Milli-Q water (18.2 MΩ cm) was used in all cases.The synthetic routes and abbreviations of target compounds are shown in Scheme 1. Generally, 2,4-dihydroxybenzaldehyde was refluxed with 1.05 mol equiv of 1-bromooctadecane and KOH in ethanol for 24 h. The ethanol was removed, and the resulting intermediate 2-hydroxyl-4-octadecyloxybenzaldehyde was subsequently purified by column chromatography (light petroleum/ethyl acetate/chloroform 30:1:5 v/v/v) as a pale solid.[51,52] The para OH group reacted predominantly with 1-bromooctadecane. The gemini amphiphiles were then obtained by the condensation of 2-hydroxyl-4-octadecyloxybenzaldehyde with the corresponding diamines in anhydrous ethanol, and the final products were recrystallized twice from ethanol solutions to give pale-yellow solids. 2-Hydroxyl-4-octadecyloxybenzaldehyde (intermediate): ^{1}H NMR (DMSO-d_6) δ 0.85 (t, CH_3, 3H), 1.24−1.27 (m, CH_2, 32H), 4.00 (t, CH_2O, 2H), 6.41−7.52 (m, C_6H_3, 3H), 10.02 (s, CH═O, 1H), 11.07 (s, OH, 1H). *N*,*N*′-Bis(4-octadecyloxy-salicylidene)-1,2-ethanediamine (BisSBC18C2): MS (MALDI-TOF, *m*/*z*) 805.3 ($C_{52}H_{88}N_2O_4$). ^{1}H NMR ($CDCl_3$) δ 0.90 (m, CH_3, 6H), 1.27−1.78 (m, CH_2, 64H), 3.86 (t, CH_2, 4H), 3.96 (t, CH_2O, 4H), 6.37−7.10 (m, C_6H_3, 6H), 8.21 (s, CH═N, 2 H), and 13.71 (s, OH, 2H). Anal. Calcd for $C_{52}H_{88}N_2O_4$: C, 77.56%; H, 11.01%; N, 3.48%. Found: C, 77.64%; H, 11.12%; N, 3.36%. *N*,*N*′-Bis(4-octadecyloxy-salicylidene)-1,4-butanediamine (BisSBC18C4): MS (MALDI-TOF, *m*/*z*) 833.4

(23) Bell, P. C.; Bergsma, M.; Dolbnya, I. P.; Bras, W.; Stuart, M. C. A.; Rowan, A. E.; Feiters, M. C.; Engberts, J. B. F. N. *J. Am. Chem. Soc.* **2003**, *125*, 1551−1558.
(24) Johnsson, M.; Wagenaar, A.; Engberts, J. B. F. N. *J. Am. Chem. Soc.* **2003**, *125*, 757−760.
(25) (a) Oda, R.; Huc, I.; Candau, S. *Chem. Commun.* **1997**, 2105. (b) Oda, R.; Huc, I.; Candau, S. J. *Angew. Chem., Int. Ed.* **1998**, *37*, 2689−2691.
(26) Estroff, L. A.; Hamilton, A. D. *Angew. Chem., Int. Ed.* **2000**, *39*, 3447−3450.
(27) Esumi, K.; Hara, J.; Aihara, N.; Usui, K.; Torigoe, K. *J. Colloid Interface Sci.* **1998**, *208*, 578.
(28) Muller, P. U.; Akpo, C. C.; Stockelhuber, K. W.; Weber, E. *Adv. Colloid Interface Sci.* **2005**, *114*, 291−302.
(29) Nishida, J.; Brizard, A.; Desbat, B.; Oda, R. *J. Colloid Interface Sci.* **2005**, *284*, 298−305.
(30) Wang, Y. J.; Desbat, B.; Manet, S.; Aime, C.; Labrot, T.; Oda, R. *J. Colloid Interface Sci.* **2005**, *283*, 555−564.
(31) Li, Z. X.; Dong, C. C.; Wang, J. B.; Thomas, R. K.; Penfold, J. *Langmuir* **2002**, *18*, 6614−6622.
(32) Seredyuk, V.; Alami, E.; Nyden, M.; Holmberg, K.; Peresypkin, A. V.; Menger, F. M. *Colloids Surf., A* **2002**, *203*, 245−258.
(33) Matti, V.; Saily, J.; Ryhanen, S. J.; Holopainen, J. M.; Borocci, S.; Mancini, G.; Kinnunen, P. K. J. *Biophys. J.* **2001**, *81*, 2135−2143.
(34) Walsh, C. B.; Wen, X. Y.; Franses, E. I. *J. Colloid Interface Sci.* **2001**, *233*, 295−305.
(35) Chierici, S.; Boullanger, P.; MarronBrignone, L.; Morelis, R. M.; Coulet, P. R. *Chem. Phys. Lipids* **1997**, *87*, 91−101.
(36) Sumida, Y.; Masuyama, A.; Oki, T.; Kida, T.; Nakatsuji, Y.; Ikeda, I.; Nojima, M. *Langmuir* **1996**, *12*, 3986−3990.
(37) Boschkova, K.; Feiler, A.; Kronberg, B.; Stalgren, J., Jr. *Langmuir* **2002**, *18*, 7930.
(38) (a) Zana, R.; Benrraou, M.; Rueff, R. *Langmuir* **1991**, *7*, 1072−1075. (b) Zana, R. *Adv. Colloid Interface Sci.* **2002**, *97*, 205.
(39) Sikiric, M.; Smit, I.; Tusek-Bozic, L.; Tomasic, V.; Pucic, I. *Langmuir* **2003**, *19*, 10044−10053.
(40) Wang, X. F.; Shen, Y. Z.; Pan, Y.; Liang, Y. Q. *Langmuir* **2001**, *17*, 3162−3167.
(41) Nieh, M.-P.; Kumar, S. K.; Ferhando, R. H. *Langmuir* **2004**, *20*, 9061−9068.
(42) Knock, M. M.; Bain, C. D. *Langmuir* **2000**, *16*, 2857−2865.
(43) Bhattacharya, S.; De, S. *Langmuir* **1995**, *11*, 3400−3410.
(44) Chen, X.; Wang, J.; Shen, N.; Luo, Y.; Li, L.; Liu, M.; Thomas, R. K. *Langmuir* **2002**, *18*, 6222−6228.
(45) (a) Zhai, X.; Zhang, L.; Liu, M. *J. Phys. Chem. B* **2004**, *108*, 7180−7185. (b) Zhai, X.; Liu, M. *J. Colloid Interface Sci.* **2006**, *295*, 181−187. (c) Jiang, M.; Zhai, X.; Liu, M. *Langmuir* **2005**, *21*, 11128−11135.
(46) (a) Rousso, L.; Friedman, N.; Sheves, M.; Ottolenghi, M. *Biochemistry* **1995**, *34*, 12059. (b) Bassov, T.; Sheves, M. *Biochemistry* **1986**, *25*, 5249.
(47) Kawamura, S.; Tsutsui, T.; Saito, S.; Murao, Y.; Kina, K. *J. Am. Chem. Soc.* **1988**, *110*, 509−511.
(48) (a) Liu, Y.; Liu, M. *Thin Solid Films* **2002**, *415*, 248. (b) Liu, Y.; Liu, M. *New J. Chem.* **2002**, *26*, 180.
(49) (a) Nagel, J.; Oertel, U.; Friedel, P.; Komber, H.; Moebius, D. *Langmuir* **1997**, *13*, 4693−4698. (b) Liu, M.; Xu, G.; Liu, Y.; Chen, Q. *Langmuir* **2001**, *17*, 427−431.
(50) Jiao, T. F.; Liu, M. *J. Phys. Chem. B* **2005**, *109*, 2532−2539.
(51) (a) Claramunt, R. M.; Forfar, I.; Cabildo, P.; Lafuencente, J.; Barbera, J.; Gimenez, R.; Elguero, J. *Heterocycles* **1999**, *51*, 751.
(52) Aiello, I.; Ghedini, M.; La Deda, M.; Pucci, D.; Francescangeli, O. *Eur. J. Inorg. Chem.* **1999**, *136*, 721372.

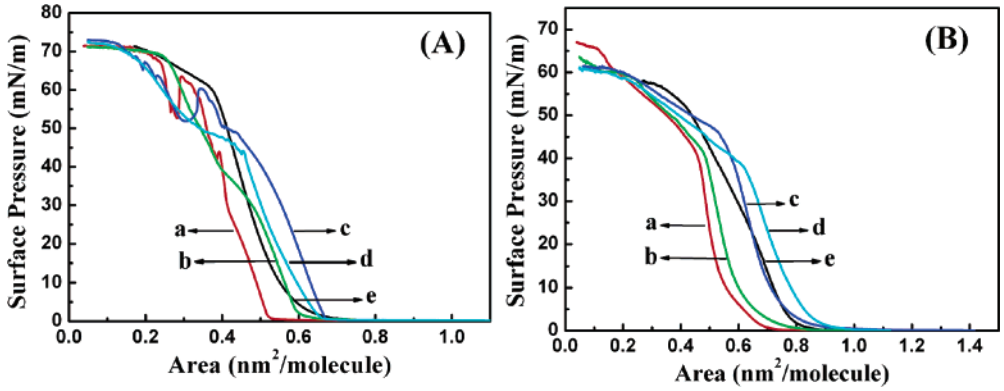

Figure 1. Surface pressure−area isotherms of gemini amphiphiles BisSBC18C*n* on the pure water surface (A) and on the subphase of a 1.0 mM $Cu(Ac)_2$ aqueous solution (B) at 20 °C: (a) BisSBC18C2, (b) BisSBC18C4, (c) BisSBC18C6, (d) BisSBC18C8, and (e) BisSBC18C10.

($C_{54}H_{92}N_2O_4$). ^{1}H NMR ($CDCl_3$) δ 0.89 (m, CH_3, 6H), 1.27−1.79 (m, CH_2, 68H), 3.59 (s, CH_2, 4H), 3.97 (t, CH_2O, 4H), 6.36−7.10 (m, C_6H_3, 6H), 8.17 (s, CH═N, 2H), 14.01 (s, OH, 2H). Anal. Calcd for $C_{54}H_{92}N_2O_4$: C, 77.83%; H, 11.13%; N, 3.36%. Found: C, 77.76%; H, 11.22%; N, 3.28%. *N*,*N*′-Bis(4-octadecyloxy-salicylidene)-1,6-hexanediamine (BisSBC18C6): MS (MALDI-TOF, *m*/*z*) 861.5 ($C_{56}H_{96}N_2O_4$). ^{1}H NMR ($CDCl_3$) δ 0.90 (m, CH_3, 6H), 1.27 (m, CH_2, 72H), 1.61−1.73 (m, CH_2, 12H), 3.54 (s, CH_2, 4H), 3.98 (t, CH_2O, 4H), 6.38−7.06 (m, C_6H_3, 6H), 8.12 (s, CH═N, 2 H), 14.06 (s, OH, 2H). Anal. Calcd for $C_{56}H_{96}N_2O_4$: C, 78.09%; H, 11.23%; N, 3.25%. Found: C, 78.02%; H, 11.32%; N, 3.33%. *N*,*N*′-Bis(4-octadecyloxy-salicylidene)-1,8-octanediamine (BisSBC18C8): MS (MALDI-TOF, *m*/*z*) 889.5 ($C_{58}H_{100}N_2O_4$). ^{1}H NMR ($CDCl_3$) δ 0.90 (m, CH_3, 6H), 1.27 (m, CH_2, 66H), 1.58−1.79 (m, CH_2, 10H), 3.52 (t, CH_2, 4H), 3.96 (t, CH_2O, 4H), 6.38−7.05 (m, C_6H_3, 6H), 8.11 (s, CH═N, 2 H), 14.15 (s, OH, 2H). Anal. Calcd for $C_{58}H_{100}N_2O_4$: C, 78.32%; H, 11.33%; N, 3.15%. Found: C, 78.46%; H, 11.42%; N, 3.23%. *N*,*N*′-Bis(4-octadecyloxy-salicylidene)-1,10-decanediamine (BisSBC18C10): MS (MALDI-TOF, *m*/*z*) 915.9 ($C_{60}H_{104}N_2O_4$). ^{1}H NMR ($CDCl_3$) δ 0.90 (m, CH_3, 6H), 1.27 (m, CH_2, 72H), 1.76 (m, CH_2, 8H), 3.53 (t, CH_2, 4H), 3.97 (t, CH_2O, 4H), 6.36−7.28 (m, C_6H_3, 6H), 8.11 (s, CH═N, 2H), 14.15 (s, OH, 2H). Anal. Calcd for $C_{60}H_{104}N_2O_4$: C, 78.55%; H, 11.43%; N, 3.05%. Found: C, 78.76%; H, 11.62%; N, 3.28%.

Procedures. The spreading monolayers of the gemini amphiphiles were formed by carefully spreading the BisSBC18C*n* solutions (ca. 0.6−0.8 mM) on a water surface. After waiting 20 min for the evaporation of the solvents, the surface pressure−area (π−A) isotherms were recorded with a compression speed of 7.5 cm^2/min at 20.0 ± 0.2 °C. In situ coordination between the gemini amphiphiles and the Cu(II) ion was performed by spreading the gemini amphiphiles on the aqueous subphase of 1 mM $Cu(Ac)_2$. This concentration of Cu(II) ions was selected in order to make the coordination complete in the spreading films. The monolayers both on water and on aqueous $Cu(Ac)_2$ were transferred by a horizontal lifting method with a unity transfer ratio onto quartz, glass, and CaF_2 plates for UV−vis, XRD, and FTIR spectral measurements, respectively. For the AFM measurement, one layer of the monolayer film was deposited onto a freshly cleaved mica plate by a vertical dipping with an upward speed of 2 mm/min. To confirm the structure of the metal complex formed in situ in the spreading films, 40-layer films were transferred onto a solid substrate, dissolved in chloroform, and then subjected to the TOF-MS measurement.

UV−vis spectra were measured with a Jasco UV-530 spectrophotometer. FTIR spectra were obtained with a Jasco FT/IR-660 plus spectrophotometer with a wavenumber resolution of 4 cm^{-1}. XRD measurements were conducted by a Rigaku D/Max-2400 X-ray diffractometer (Japan) with Cu Kα radiation (λ = 0.154 nm) with an angle resolution of 0.02°. AFM measurements were made in tapping mode (Nanoscope IIIa multimode system, Digital Instruments, Santa Barbara, CA) with silicon cantilever probes. All AFM images are shown in the height mode without any image processing except flattening. ^{1}H NMR spectra were obtained on an ARX400 (Bruker) NMR spectrometer in $CDCl_3$ or DMSO-d_6 with TMS as an internal standard. MALDI-TOF mass spectra were determined with BIFLEXIII. Elemental analysis was carried out with a Flash EA Carlo-Erba-1106 Thermo-Quest. The molecular simulation and limiting area calculation were obtained from PCMODEL version 6.0 and ChemOffice version 2004 from the CambridgeSoft Corporation.

Results

Monolayer Formation of Gemini Amphiphiles at the Air/Water Interface. Figure 1 shows the surface pressure−area (π−A) isotherms of monolayers of gemini amphiphiles under different conditions. Although the shapes of these curves are similar, the isotherms showed clear differences in interfacial properties such as limiting molecular areas and transition points depending on both the spacer length and the subphase.

On the water surface, BisBSC18C2 shows the onset of surface pressure at ca. 0.52 nm^2/molecule. Then the surface pressure shows a linear increase below a pressure of 30 mN/m, and a phase transition is observed at about 30 mN/m, which is related to the film changing into a solid condensed state. After that point, the film shows a second mound at around 45 mN/m. This mound was found to diminish with decreasing compression speed, indicating that the mound is due to a kinetic effect.[53]

In addition, with the increment of the spacer length in the gemini amphiphiles, the onset of surface pressure showed a slight shift to larger molecular areas, and there was also a slight increase in the transition surface pressure of the monolayers. When the spacer length increased to C10, the transition regions disappeared. However, the extrapolated limiting areas from the linear part of the isotherms to zero surface pressure fell into the range of 0.52−0.67 nm^2/molecule for all gemini amphiphile monolayers. On the basis of the CPK model, the molecule was simplified as a rectangular box, and the limiting areas were estimated by multiplying the side of the aromatic ring and the length between the two headgroups. Limiting areas ranging from 0.56 to 1.02 nm^2/molecule were estimated by assuming that the spacers in the amphiphiles were parallel to the water surface. Both the estimated limiting areas and the experimentally measured ones are listed in Table 1.

From Table 1, it is clear that the experimental and estimated values are in agreement for BisSBC18C2 and C4 amphiphiles. A larger deviation is observed for others with longer spacers. The estimated values of the limiting molecular areas are always larger than the experimentally measured ones. Moreover, it is interesting that the limiting areas showed a maximum at a spacer

(53) Fujita, K.; Kimura, S.; Imanishi, Y.; Rump, E.; Ringsdorf, H. *Langmuir* **1994**, *10*, 2731.

Table 1. Experimental and Estimated Limiting Molecular Areas of BisSBC18C*n* Films on Water and the Aqueous $Cu(Ac)_2$ Subphase

properties	BisSBC18C*n*				
	$n = 2$	$n = 4$	$n = 6$	$n = 8$	$n = 10$
molecular area (nm^2) (water, expt)	0.52	0.60	0.67	0.59	0.55
molecular area (nm^2) (water, calcd)	0.56	0.69	0.82	0.96	1.02
molecular area (nm^2) (Cu, expt)	0.54	0.62	0.71	0.82	0.80
molecular area (nm^2) (Cu, calcd)	0.60	0.71	0.79	0.78	0.75

length of C6 for the monolayers on the water surface. After C6, the molecular areas decreased. This phenomenon is very similar to that for our previously reported gemini/DNA monolayers,[44] where a maximum limiting molecular area was observed for the complex gemini monolayer having a hexamethylene spacer. In the present case, a similar explanation can be applied. That is, when the spacer length in the gemini amphiphiles is longer than C6, the alkyl spacer will curve upward and the limiting area will subsequently decrease. When the gemini amphiphiles are spread on the subphase containing $Cu(Ac)_2$, significant differences are observed. First, no transition point is observed for most of the monolayers except for BisSBC18C10, which showed an ambiguous transition from 25 mN/m. Second, both the onset of surface pressure and the extrapolating molecular areas become larger in comparison with those of the corresponding monolayers on the water surface. It is well known that Schiff base derivatives are easy to coordinate with transition-metal ions. The present result implies that the gemini-type Schiff base amphiphiles react with Cu(II) ions in the spreading monolayers. Table 1 also lists the experimental and estimated values of the limiting molecular areas for the gemini/Cu(II) complex films by assuming that the Schiff base amphiphiles form intramolecular complexes with Cu(II) ions. In the process of complex formation, the alkyl spacer may curve. Therefore, the estimated values from the CPK model are smaller than those on the water surface. However, the experimental limiting area values also show a maximum against the spacer length. However, in this case, the maximum limiting area is observed for the gemini amphiphile with a spacer length of C8. This indicates that in situ coordination could induce a slightly different conformation change in the alkyl spacer in the complex films.

Characterization of the Transferred Films. *UV−Vis Spectra of the Transferred Films.* The spreading films both on water and on the aqueous $Cu(Ac)_2$ subphase were transferred onto solid substrates, and their UV−vis spectra were measured. Figure 2 shows the UV−vis spectra of the multilayer films transferred from water and the Cu(II) ion subphase in comparison with those in ethanol solution. In ethanol solution, the absorption peaks appear at around 272, 305, and 378 nm with only a small shift for the amphiphiles with different spacer lengths. The former two bands can be ascribed to the localized absorption of the aromatic moieties whereas the latter can be attributed to the charge-transfer transition.[54] As for the spectra of LB films, significant changes in the absorption bands are observed. First, the charge-transfer band at around 378 nm in solution becomes vague in the films whereas the bands at 272 and 305 nm show slight red shifts to 276 and 308 nm, respectively. These red shifts in the UV−vis spectra of the LB films in comparison with those in solution are generally related to the ordered packing of the molecules in the LB films. Second, two clear split absorptions are observed at around 238 and 246 nm, which were involved in the $\pi-\pi^*$ transition of the localized aromatic ring.[55] With the increment in the spacer length, the relative intensity of the two bands changed greatly, as shown in the plot. In the case of BisSBC18C2, only one band is observed at 238 nm. With the spacer length increase, the band at 246 nm became stronger. The split of this band suggests that there exists a strong interaction between neighboring Schiff bases.

When the films were deposited from the aqueous $Cu(Ac)_2$ subphase, the absorption bands shifted to new positions of 286 and 351 nm, respectively. In addition, we have seen some strong absorption bands at around 240 nm. These changes suggest that coordination occurred between the Schiff base compounds and the Cu(II) ions in the subphase. It is also noted that the absorption spectrum of the BisSBC18C2/Cu(II) complex film has a small shift in comparison with those of other amphiphiles, implying that the BisSBC18C2/Cu(II) complex films may be different from the films fabricated from other gemini amphiphiles. To confirm the in situ coordination between the Schiff base and the metal ions and to disclose the structure of the formed metal complexes, the transferred multilayers films on the $Cu(Ac)_2$ subphase were dissolved in chloroform, and their molecular weights were measured by TOF-MS. The MS results (Supporting Information) verified the formation of the 1:1 ligand/Cu(II) ion complex. In the BisSBC18C2/Cu(II) ion complex, an additional peak ascribed to the 2:2 ligand/Cu(II) complex (Supporting Information) was also observed. These results strongly support the above deduction from the $\pi-A$ isotherms and UV−vis spectra.

FTIR Spectra of the Transferred Films. FTIR spectroscopy is a powerful technique for detecting vibration changes during molecular interactions. This method is particularly useful for those systems where reaction occurs. Figure 3 shows the FTIR spectra of the deposited LB films from water and the aqueous Cu(II) ion subphase.

For films transferred from the water surface, typical vibrations of Schiff base were observed. For example, strong characteristic vibrational peaks ascribed to the C═N bond were observed at 1625 cm^{-1} for all of the films. Generally, the C═N bond appeared at 1640 cm^{-1}. In the present case, the lower frequencies suggest that these groups form strong hydrogen bonds with the adjacent hydroxy groups.[56,57] In addition, other strong vibrations at 1575, 1522, and 1302 cm^{-1} are also observed and can be assigned to the conjugate aromatic moieties and phenolic group in the amphiphiles.[58] However, strong peaks of the alkyl spacer and the alkyl chains are clearly observed at 2919, 2850, and 1470 cm^{-1} and are assigned to the asymmetric and symmetric stretching and scissor vibrations of methylene chains, respectively. It is well known that appearance of the CH_2 asymmetric and symmetric stretching bands at lower wavenumbers (ca. 2918 and 2848 cm^{-1}, respectively) indicates a highly ordered and well-organized arrangement of the hydrocarbon chains whereas their appearance at higher wavenumbers is indicative of the increase in conformational disorder in the hydrocarbon chains.[59,60] In present case, the vibrational position of the films suggests that the alkyl chains

(54) Chichak, K.; Jacquemard, U.; Branda, N. R. *Eur. J. Inorg. Chem.* **2002**, 357−368.

(55) Issa, R. M.; Khedr, A. M.; Rizk, H. F. *Spectrochim. Acta, Part A* **2005**, *62*, 621−629.

(56) Hoshino, N.; Inabe, T.; Mitani, T.; Maruyama, Y. *Bull. Chem. Soc. Jpn.* **1988**, *61*, 4207.

(57) Kamata, T.; Umemura, J.; Takenaka, T.; Koizumi, N. *J. Phys. Chem.* **1991**, *95*, 4096.

(58) (a) Pang, S. F.; Liang, Y. Q. *Spectrochim. Acta, Part A* **2001**, *57*, 435−439. (b) Pang, S. F.; Liang, Y. Q. *Mater. Chem. Phys.* **2001**, *71*, 103−106. (c) Pang, S. F.; Ye, Z. F.; Li, C.; Liang, Y. Q. *J. Colloid Interface Sci.* **2001**, *240*, 480−486.

(59) Umemura, J.; Cameron, D. G.; Mantsch, H. H. *Biochim. Biophys. Acta* **1980**, *602*, 32.

(60) Cameron, D. G.; Martin, A.; Moffatt, D. J.; Mantsch, H. H. *Biochemistry* **1985**, *24*, 4355.

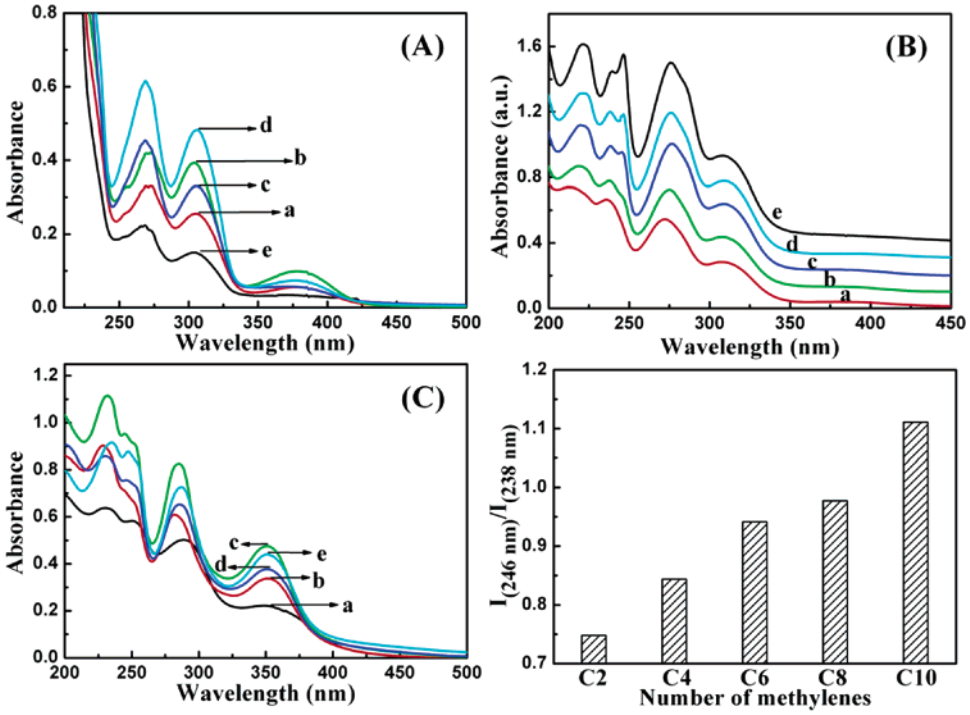

Figure 2. UV−vis spectra of amphiphilic BisSBC18C*n*/ethanol solutions (A); 40-layer multilayer films deposited from the water surface (B) and from the subphase of a 1.0 mM $Cu(Ac)_2$ solution (C) at 30 mN/m: (a) BisSBC18C2, (b) BisSBC18C4, (c) BisSBC18C6, (d) BisSBC18C8, and (e) BisSBC18C10. The plot is the relative intensity ratio of absorption peaks at 246 vs 238 nm in B as a function of spacer length.

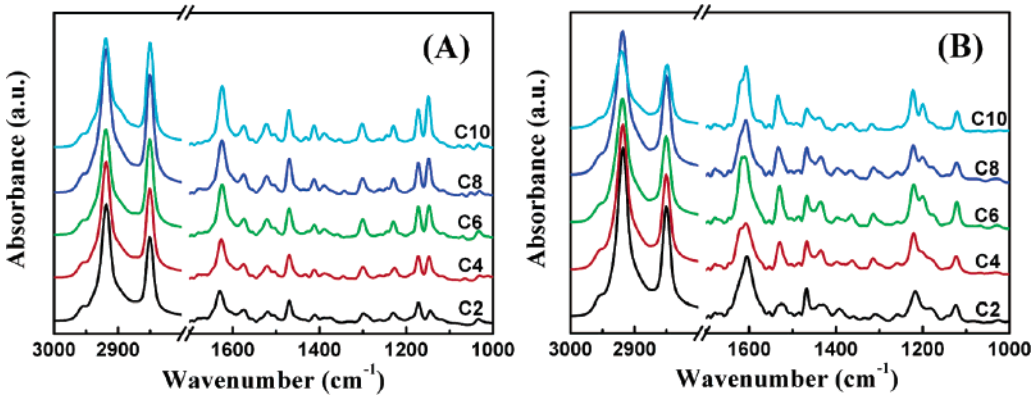

Figure 3. FTIR spectra of 80-layer BisSBC18C*n* multilayer films transferred from the water surface (A) and the subphase of a $Cu(Ac)_2$ solution (B) at 30 mN/m.

in the films are basically in an ordered packing. It is also noted that with the increment of the spacer length the relative intensity of the peak from 2919 to 2850 cm^{-1} decreases. Although the vibrational intensity at 2919 cm^{-1} is stronger than that at 2850 cm^{-1} for BisSBC18C2 multilayer films, the intensities became nearly the same for BisSBC18C10 films. It is generally assumed that when the relative intensity of the asymmetric CH_2 to symmetric vibration decreases, the alkyl chain tends to incline to the film plane.[61] However, in our present system, the case is different. Because both the alkyl chain and the polymethylene spacer contribute to the vibrational bands simultaneously, the change in the relative intensity could not be wholly ascribed to the tilting of the alkyl chains. In fact, the direction of the polymethylene spacer is perpendicular to the alkyl chain. With the spacer increased, more polymethylene groups in the gemini films will contribute to the vibration at 2850 cm^{-1}, resulting in an increment of the intensity at 2850 cm^{-1}. Therefore, the decrease in the relative intensity of the peak from 2919 to 2850 cm^{-1} with the increment in the spacer length seems to be mainly due to the contribution from the CH_2 vibration of the spacer although we cannot completely exclude the effect of the tilting of the alkyl chain.

When the films were deposited from the subphase of Cu(II) ions, clear spectral changes in comparison with those on the water surface were observed, confirming the coordination of the Schiff bases with Cu(II) ions. The strong C═N vibration shifted to 1607 cm^{-1}, and the original band at 1575 shifted to 1534 cm^{-1}. Another characteristic change is the shift from 1302 to 1317 cm^{-1} for the phenolic group. However, no obvious shift in the position of the CH_2 vibration or the relative intensity of the asymmetric and symmetric CH_2 vibrations was observed with the increment in the spacer length.

AFM Measurements. To gain further insight into the assembly structure of the gemini amphiphiles at the air/water interface, one layer of the spreading films was transferred onto a newly cleaved mica surface, and the surface morphology was measured

(61) (a) Terashita, S.; Ozaki, Y.; Iriyama, K. *J. Phys. Chem.* **1993**, *97*, 10445. (b) Nakagoshi, A.; Wang, Y.; Ozaki, Y.; Iriyama, K. *Langmuir* **1995**, *11*, 3614.

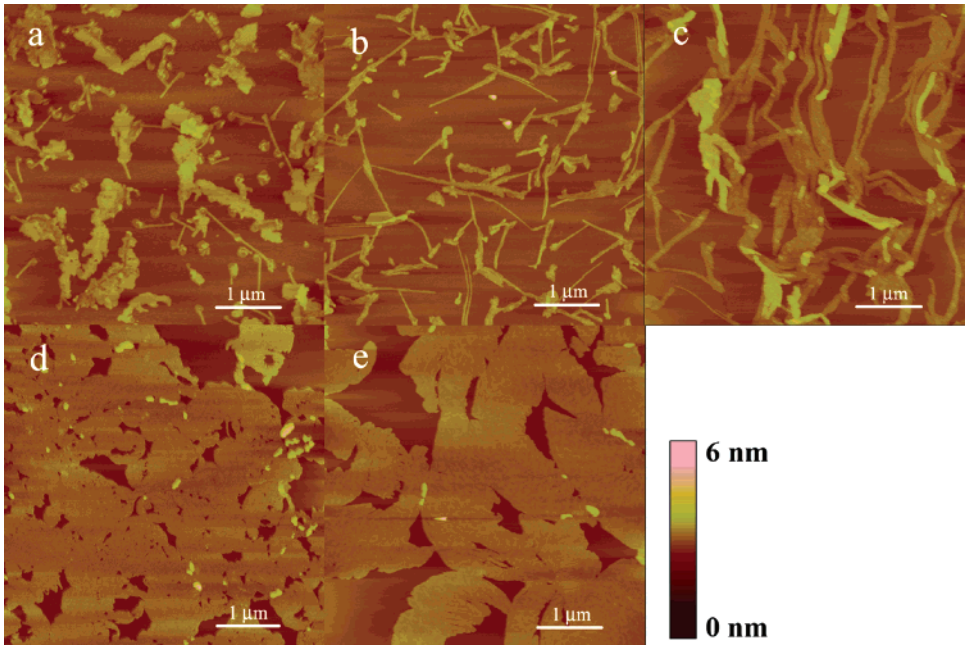

Figure 4. AFM images of one-layer BisSBC18C*n* LB films deposited from the water surface at 20 mN/m: (a) BisSBC18C2, (b) BisSBC18C4, (c) BisSBC18C6, (d) BisSBC18C8, and (e) BisSBC18C10.

Table 2. Layer Distances of BisSBC18C*n* Films on Water and the Aqueous $Cu(Ac)_2$ Subphase and Comparison with the Average Heights from AFM Measurements

		BisSBC18C*n*				
layer distance		$n = 2$	$n = 4$	$n = 6$	$n = 8$	$n = 10$
water subphase (nm)	XRD	3.62	3.68	3.74	3.91	4.09
	AFM	6.9 ± 0.2	3.7 ± 0.2	3.8 ± 0.1	4.0 ± 0.1	4.1 ± 0.1
Cu(II) subphase (nm)	XRD	3.48	3.48	3.56	3.62	3.66
	AFM)	3.2 ± 0.2	3.3 ± 0.2	3.4 ± 0.2	3.5 ± 0.2	3.6 ± 0.2

with AFM. Figure 4 shows the AFM pictures of the BisSBC18C*n* LB film from the water surface.

For the BisSBC18C2 film on the water surface, domains including irregular aggregates and blocks with some nanorods could be found in Figure 4a. Depending on the spacer length of the gemini amphiphiles, different morphologies were obtained. Nanonail-like and nanotape-like morphologies were observed for BisSBC18C4 and BisSBC18C6, respectively. The nails and tapes were extended to several micrometers, and the widths were 70 ± 20 and 150 ± 30 nm, respectively. When the spacer length increased to C8 and C10, larger blocks were formed. However, the section analysis shows that the average height of all of the AFM pictures ranged from 3.7 to 4.1 nm with the exception of BisSBC18C2, which is about 7.1 nm, as listed in Table 2.

However, when the Cu(II) ion was added to the subphase, the interfacial morphologies changed significantly in comparison with those on the water surface. As for the BisSBC18C2 films on the Cu(II) ion subphase, a flat film with some holes was clearly observed. When the spacer length increased to four methylenes, cracks in the films were observed. For the Cu(II)-complexed film of BisSBC18C6, a clearly different rough morphology was observed in which many granular domains were observed. Wormlike fibers were observed for BisSBC18C8 and BisSBC18C10. Although the morphologies were very similar for the two films, the latter with a width of 35 ± 4 nm is thicker than the former. The section analysis showed that all of these films have an average height range from 3.2 to 3.6 nm.

XRD Spectra of the Transferred Film. To characterize the layer structures of the deposited LB films, X-ray diffraction (XRD) spectra of the transferred BisSBC18C*n* multilayer films from water and the Cu(II) subphase were obtained, as shown in Figure 6. One to two peaks were observed for the transferred LB films. According to Bragg's equation, the layer distances of the gemini amphiphiles can be estimated and are listed in Table 2. It is observed that with the increment of methylene in the spacer the layer distance increased for the films both from the water surface and from the aqueous $Cu(Ac)_2$ subphase.

Discussion

All of the above data indicate that this new series of gemini amphiphiles shows not only similar properties to those of gemini monolayers but also new features.

First, a clear spacer effect was observed for the spreading monolayers of this series of gemini amphiphiles on either water or the aqueous $Cu(Ac)_2$ subphase. The limiting molecular areas of the monolayers on both water and the $Cu(Ac)_2$ subphase showed a maximum at a certain spacer length. For the amphiphile with a relatively short spacer, the spacer was suggested to be parallel to the water surface. With the increment in length, the spacer could take a gauche conformation and curve upward, as illustrated in Scheme 2. Therefore, we observed that the limiting molecular areas first increased with spacer length and then decreased for the longer spacer. The maximum limiting molecular areas were observed at spacer lengths of C6 and C8 for the films on water and $Cu(Ac)_2$, respectively. This phenomenon is similar to our previous results for bolaamphiphiles and gemini-type amphiphiles[44,50] and seemed to be a general rule for the gemini amphiphiles with a hydrophobic spacer. The slight differences in the molecular areas and the maximum in the gemini monolayers on water from those on the $Cu(Ac)_2$ subphase are suggested to be due to the coordination between the Schiff base and Cu(II). It seems that the coordination geometry of the complex makes the conformation of the polymethylene spacer in the complex more fixed and more difficult to change.

Second, the multilayer films showed special features in their layer structure. From the XRD of the films, a layer distance between 3.5 and 4.1 nm was obtained for the multilayer films. In addition, the XRD showed an increase in the layer distance with spacer length. If we assume that both the alkyl chain and

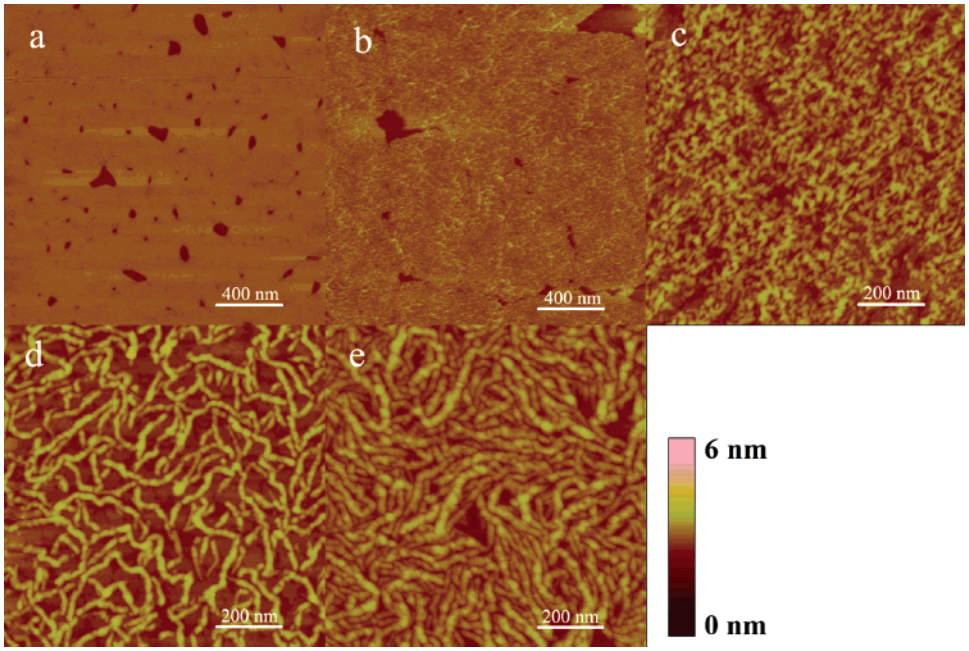

Figure 5. AFM images of one-layer BisSBC18C*n* LB films deposited from the subphase of a 1.0 mM $Cu(Ac)_2$ solution at 20 mN/m: (a) BisSBC18C2, (b) BisSBC18C4, (c) BisSBC18C6, (d) BisSBC18C8, and (e) BisSBC18C10.

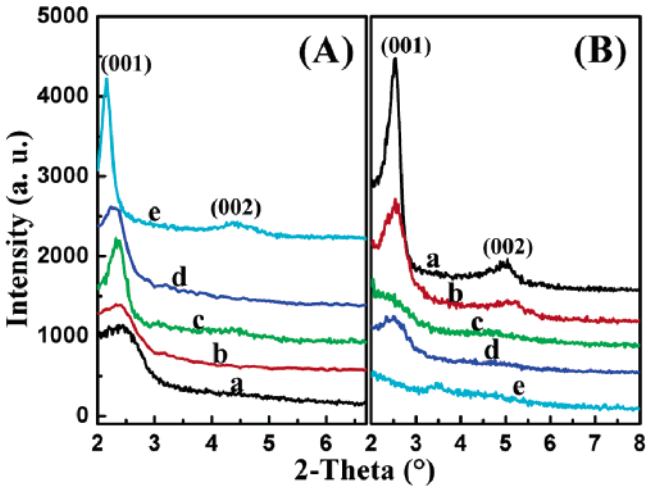

Figure 6. XRD spectra of BisSBC18C*n* multilayer films deposited from the water surface (A) and the subphase of a 1.0 mM $Cu(Ac)_2$ solution (B) at 20 mN/m: (a) BisSBC18C2, (b) BisSBC18C4, (c) BisSBC18C6, (d) BisSBC18C8, and (e) BisSBC18C10.

the Schiff base moiety are vertical to the solid substrate with the spacer parallel to the film plane, then a maximum thickness of 3.3 nm can be estimated for the gemini films, regardless of the spacer length. This obviously excluded the X-type or Z-type film structure in the multilayer films. Two possible Y-type arrangements of the molecules could be considered. One is the bilayer structure, and the other is the interdigitated structures. For the bilayer structure, to obtain a layer distance of 3.5 nm for BisSBC18C2, the alkyl chain should incline 36° to the film plane. However, this is contrary to the FTIR spectrum, which indicated that the alkyl chain is rather inclined to the film normal than the film plane because the vibrational intensity at 2919 cm^{-1} is stronger than that at 2850 cm^{-1}. Therefore, the more plausible explanation for the film structure is that the gemini amphiphiles formed an interdigitated Y-type film, as shown in Scheme 2. Previously, it was reported that similar interdigitated multilayers were obtained in several films from conventional amphiphiles.[62,63] For gemini-type monolayers, this is more plausible because the two alkyl chains were separated by a hydrophobic spacer. In

Scheme 2. Schematic Illustration of the Packing Modes of BisSBC18C*n* in Organized Films[a]

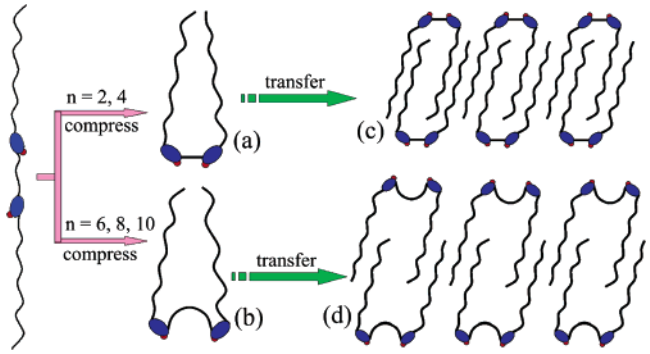

[a] When compressed at the air/water interface, the spacers are parallel to the water surface for a short spacer (a) and have an upward-curved conformation with a longer spacer (b). During the transfer process, the overturning of the film leads to the formation of interdigitated films (c and d for different spacer lengths).

particular, when the spacer is longer, the alkyl chains of the neighboring molecules will be able to penetrate easily into the empty place between the alkyl chains in another layer. With such a structure, the layer distance will increase when the spacer length increases. For the film with a short spacer, because the spacer is parallel to the film plane, the alkyl chain can penetrate deeply into the space between the two alkyl chains, and the layer distance is short, as shown in Scheme 2c. As the spacer length increases, the spacer can be curved upward between the two neighboring alkyl chains in the gemini molecule, and the alkyl chains from another molecule cannot penetrate as deeply, as shown in Scheme 2d. Thus, we obtained increased layer distances. In addition, it is natural to assume that the film will become loosely packed when the spacer increases if the film takes such a structure. This is supported by the XRD in which the half width of the diffraction peak broadened when the spacer length increased.

(62) Alonso, C.; Kuzmenko, I.; Jensen, T. R.; Kjaer, K.; Lahav, M.; Leiserowitz, L. *J. Phys. Chem. B* **2001**, *105*, 8563.
(63) Osman, M. A.; Ploetze, M.; Skrabal, P. *J. Phys. Chem. B* **2004**, *108*, 2580−2588.

It was suggested that such a multilayer structure was formed during the film transfer in which "overturning" could possibly occur.[64] It seems that such overturning could easily occur for the present monolayers of the gemini amphiphiles. We have transferred a one-layer LB film using both vertical and horizontal methods for AFM measurements. A similar film thickness ranging from 3.3 to 4.1 nm, which corresponds to the XRD results as shown in Table 2, was obtained. We have noticed that the BisSBC18C2 film on water forms as an even thicker film than the other films. This can be suggested to be due to the further overlapping of the basic interdigitated bilayer film. It was further suggested that such an interdigitation alignment of the alkyl chains in the transferred films was due to the hydrophobic spacer and the relatively rigid headgroup in the Schiff base gemini-type amphiphiles. Previously, we observed that only a Z-type film was obtained for a gemini/POM system and that the same layer distances were obtained regardless of the spacer.[45c]

Third, the covalently linked spacer to the Schiff base headgroups caused a further change in the packing of the aromatic rings. From the UV−vis spectra, two absorption bands assigned to the localized $\pi-\pi^*$ transition were observed at 238 and 246 nm. These two bands were supposed to be due to the aggregation of the aromatic ring in H and J aggregates, respectively. When the alkyl chain was short, an H aggregation of the aromatic ring was predominant. When the spacer length increased, the J aggregation was preferred. Such packing changes were clearly verified in the FTIR spectra, where asymmetric and symmetric vibrations of C−O, which are related to the alkyloxy groups connecting to the aromatic ring, were observed at 1172 and 1149 cm^{-1}, respectively. With the increment in spacer length, the symmetric vibration increased, indicating that the alkyloxy chain was more inclined. This is in agreement with the UV spectra, which suggest that with the spacer length increase the aromatic ring tends to prefer to J aggregation. For the Cu(II)-complexed films, because the aromatic rings as well as the conjugated C═N group are coordinated with Cu(II), no such change in the packing could be observed.

(64) Corkery, R. W. *Langmuir* **1997**, *13*, 3592.

Conclusions

The newly designed gemini-type amphiphile containing Schiff base groups can form stable monolayers at the air/water interface. They can coordinate with Cu(II) ions in situ at the air/water interface and form an intramolecular complex between the ligand and the metal ion. For BisSBC18C2, an additional intermolecular dimerlike complex could be formed also. The series of amphiphiles shows a strong spacer effect on both the interfacial properties and the assemblies. Maximum limiting molecular areas are observed for the monolayers of the gemini amphiphiles with spacer lengths of C6 and C8 on water and aqueous $Cu(Ac)_2$, respectively, which is due to the formation of the upward-curved conformation of the hydrophobic spacer. Such an effect of the spacer leads to different morphologies such as nanonail and wormlike nanoarchitectures, depending on the spacer length and the subphases. Because of the covalent connection of the Schiff base groups by the alkyl spacer, the $\pi-\pi^*$ absorption of the localized aromatic rings split into two bands that could be assigned to H and J aggregation, respectively. With the spacer length increased, the J aggregation of the aromatic ring seems to be preferred. An interdigitated bilayer structure is formed in the multilayer films both for the film from water and from the aqueous $Cu(Ac)_2$ subphase. The present work provided new insight into the design and interfacial assembly of the gemini amphiphiles.

Acknowledgment. This work was supported by the National Natural Science Foundation of China (nos. 20533050 and 90306002), the Basic Research Development Program (2005CCA06600), and the Fund of the Chinese Academy of Sciences.

Supporting Information Available: TOF-MS spectra of metal complexes formed through in situ coordination. This material is available free of charge via the Internet at http://pubs.acs.org.

LA060343W